

REPORT DOCUMENTATION PAGE					Form Approved OMB No. 0704-0188	
<p>The public reporting burden for this collection of information is estimated to average 1 hour per response, including the time for reviewing instructions, searching existing data sources, gathering and maintaining the data needed, and completing and reviewing the collection of information. Send comments regarding this burden estimate or any other aspect of this collection of information, including suggestions for reducing the burden, to Department of Defense, Washington Headquarters Services, Directorate for Information Operations and Reports (0704-0188), 1215 Jefferson Davis Highway, Suite 1204, Arlington, VA 22202-4302. Respondents should be aware that notwithstanding any other provision of law, no person shall be subject to any penalty for failing to comply with a collection of information if it does not display a currently valid OMB control number.</p> <p>PLEASE DO NOT RETURN YOUR FORM TO THE ABOVE ADDRESS.</p>						
1. REPORT DATE (DD-MM-YYYY) 20-07-2004		2. REPORT TYPE Conference Proceedings		3. DATES COVERED (From - To) 20 Jul 2004 - 24 Jul 2004		
4. TITLE AND SUBTITLE Blast-Resistant Window Concepts			5a. CONTRACT NUMBER F08637-98-C-6001 5b. GRANT NUMBER 5c. PROGRAM ELEMENT NUMBER 62201F 5d. PROJECT NUMBER 5e. TASK NUMBER 5f. WORK UNIT NUMBER 4397D11E			
6. AUTHOR(S) William Stanley Strickland, Mark Anderson			8. PERFORMING ORGANIZATION REPORT NUMBER AFRL-ML-TY-TP-2003-4532			
7. PERFORMING ORGANIZATION NAME(S) AND ADDRESS(ES) Air Force Research Laboratory Airbase Technologies Division 139 Barnes Drive, Suite 2 Tyndall AFB FL 32403-5323			10. SPONSOR/MONITOR'S ACRONYM(S)			
9. SPONSORING/MONITORING AGENCY NAME(S) AND ADDRESS(ES)			11. SPONSOR/MONITOR'S REPORT NUMBER(S)			
12. DISTRIBUTION/AVAILABILITY STATEMENT Distribution Statement "A". Distribution Unlimited						
13. SUPPLEMENTARY NOTES Published in ASME Pressure Vessels and Piping Conf 2003 PVP2003-1831						
14. ABSTRACT Terrorist bombs threaten American civilians and military personnel both at home and abroad. Analysis of data from previous terror attacks indicates the largest number of injuries result from projected glass shards from shattered windows and facades. Three key issues have led to increased interest in new window materials, as well as changes in building design codes: (1) actual terror attacks; (2) the threat of future terror attacks; and (3) monetary losses due to hurricanes. New protective products include a wide variation of films and laminated glasses for retrofit/replacement. Air Force Research Laboratory (AFRL) research has shown that these protective films will reduce the fragmentation of the enclosed glass. However, protective films that are not anchored will not provide retention of the film/glass system under the severe blast loadings expected from terror bombs.						
15. SUBJECT TERMS						
16. SECURITY CLASSIFICATION OF: a. REPORT U b. ABSTRACT U c. THIS PAGE U			17. LIMITATION OF ABSTRACT SAR	18. NUMBER OF PAGES 10	19a. NAME OF RESPONSIBLE PERSON Stan Strickland 19b. TELEPHONE NUMBER (Include area code) 850-283-9709	

DISTRIBUTION STATEMENT A
Approved for Public Release
Distribution Unlimited

Proceedings of PVP2003
2003 ASME Pressure Vessels and Piping Conference
July 20-24, 2003 Cleveland Ohio, USA

PVP2003-1831

BLAST-RESISTANT WINDOW CONCEPTS

W.S. Strickland
Air Force Research Laboratory
Deployed Systems Branch
(AFRL / MLQD)
Tyndall AFB, FL 32403
Stan.Strickland@Tyndall.AF.Mil

Mark Anderson, Ph.D., P.E.
Applied Research Associates, Inc.
Engineering Science Division
(supporting AFRL / MLQD)
Tyndall AFB, FL 32403
Mark.Anderson@Tyndall.AF.Mil

Maj. Dov Dover, P.E.
Israeli Air Force
Exchange Officer
(on assignment to AFRL / MLQD)
Tyndall AFB, FL 32403
Dover@Gulf.net

ABSTRACT

Terrorist bombs threaten American civilians and military personnel both at home and abroad. Analysis of data from previous terror attacks indicates the largest number of injuries result from projected glass shards from shattered windows and facades. Three key issues have led to increased interest in new window materials, as well as changes in building design codes: (1) actual terror attacks; (2) the threat of future terror attacks; and (3) monetary losses due to hurricanes. New protective products include a wide variation of films and laminated glasses for retrofit / replacement. Air Force Research Laboratory (AFRL) research has shown that these protective films will reduce the fragmentation of the enclosed glass. However, protective films that are not anchored will not provide retention of the film/glass system under the severe blast loadings expected from terror bombs.

The paper introduces the Flex window, a patent-pending blast-resistant window developed at AFRL, along with key design concepts. In addition, the paper presents results from actual blast tests of the Flex window. Tabular data and photo-documentation is used to illustrate the ability of the Flex window to handle blast pressures a full order of magnitude greater than the typical commercial "blast proof" window. New AFRL methods for modeling both exterior and interior loading functions are presented. In addition, possible response modes are discussed, based on observations of high-speed video recordings.

BACKGROUND

Glass windows and facades have been a common part of structures for hundreds of years, for visibility, and for other reasons, such as: (1) energy savings (e.g., use of ambient lighting); (2) marketing (i.e., for display of merchandise); and (3) psychology (e.g., for improved worker performance). But, even with all its positives, glass is a structurally undesirable material for severe loading from such sources as wind, projectiles, blasts, sonic booms, and earthquakes. Damage assessments from hurricanes, terrorist car bombs, and terrorist suicide bombs

have routinely pointed to projected glass as a key cause of injury and property damage. The recent increase in acts of terror has prompted research and development efforts on blast-resistant window designs to reduce injuries from flying glass, both for new construction and retrofit. New materials such as laminated glass and polymer films are appearing on the commercial market, but research at AFRL has clearly shown that these products may, in some cases, promote a false sense of security. This is dramatically illustrated in Figure 1, which is a single high-speed video frame (Anderson and Dover [1]). This figure shows two Flex windows (Flex windows are described in subsequent sections), under simultaneous blast loading. The two windows are protected on both sides with anchored polymer films, and are identical except that the window on the left has one of the laminated panels removed. Since the films are anchored, this represents a "best-case" scenario for single pane protection. The films do provide benefit, i.e., the single-panel window essentially stays in one piece – however, that single piece becomes a very dangerous projectile.



(a) films alone (b) films + damping chamber

Figure 1. Simultaneous test of Targets 1 and 2

INTRODUCTION

The protection of personnel and materials from bomb blasts has historically been achieved through the design of hardened facilities, typically on military installations. In general, these structures were reinforced concrete buildings, either partly or completely buried, and normally without any windows. In recent years, the expeditionary nature of our military actions has forced military personnel

20050119 005

to use deployable shelters and/or host nation facilities. This, in turn, creates a need for retrofit technologies that will "harden" mobile and existing facilities, particularly buildings with masonry block wall construction (common in much of the world). AFRL has developed methods of retrofitting such facilities using ESC¹ that have been proven to reduce damage and limit breaching of structures (often increasing protection levels by a factor of two). The basic technique applies an elastomeric material to internal walls of the structures, creating a membrane that absorbs the blast energy, allowing walls to "give but not break." A similar concept has been applied to windows using transparent plastic films to create the membrane effect. While commercial films are available for this application, the effectiveness of this technology has generally been limited to relatively low blast pressures (on the order of 10 psi or less), due to the problem previously illustrated in Figure 1. A new window system is presented which uses engineering mechanics to address the most difficult issue for these film-reinforced windows, i.e., keeping the whole window from becoming a projectile.

THE FLEX WINDOW

AFRL has developed a patent-pending window system which has become known by its performance-oriented nickname, the "Flex" window². The Flex window implements several dramatic improvements over previous AFRL blast-resistant windows (developed in the 1990s). The step-by-step developments which led to the Flex windows have been described elsewhere, and will not be repeated herein (see Dover, et al. [4]).

FLEX WINDOW SCHEMATIC

Figure 2 is a schematic of the Flex window, which is composed of six major components: (1) double panels (glass and film laminate assemblies); (2) damping chamber; (3) rigid metal frame; (4) rigid window frame; (5) film anchoring system; and (6) air vents (pressure relief). When the blast wave impacts the front panel, the incident pressure bends the panel inward. The use of an elastic anchoring system, coupled with the elasticity/plasticity of judiciously placed films allows the window to bow (i.e., act like a membrane). Additionally, the damping chamber traps air between the panels, so the air is both compressed and vented. The result is a system that acts as an air-spring for the front panel, reduces the pressure transferred to the back panel, and allows the two panels to oscillate at a controlled maximum amplitude, with exponential amplitude decay.

¹See Dover, et al. 2002 [3] for a full description of Elastomer Sprayed Coating, or "ESC."

²The formal name of the Flex window is "Blast Proof Window Systems with Damping ChamberTM."

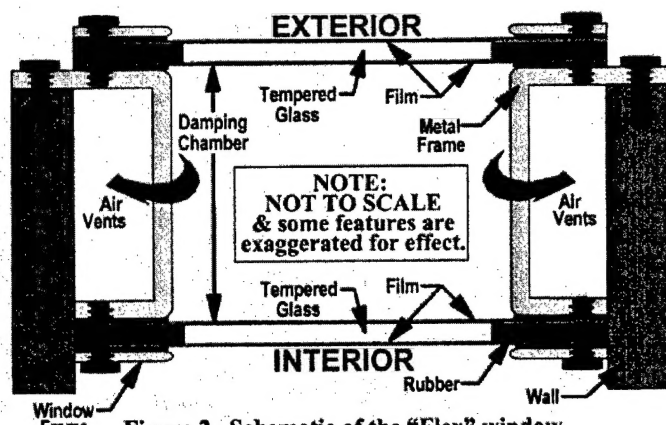


Figure 2. Schematic of the "Flex" window

DAMPING CHAMBER CONCEPT

The "damping chamber" is a vented air gap between the front and back panels of a "double panel" window that improves the blast resistance by "cushioning" the blast wave. The damping effect is sometimes easier to understand by considering the opposite, or unvented, case. If a double panel window is not vented, the front panel tends to deform inward under the incident pressure. As the front panel moves inward, the air trapped within the window compresses, applying pressure to the back panel. However, when the air gap is vented through holes in the window frame, the specific impulse transmitted to the back panel is reduced. That is, pushing air out the vents reduces the internal pressure, which, in turn, reduces the pressure transferred to the back panel. At the same time, the internal pressure build-up acts as an "air spring" against the front panel, tending to reduce its momentum. This combined effect is similar to the damping of highway crash barrels used to protect automobiles in collisions with highway barriers, or the damping of an air bag used by stunt men to fall from great heights without serious injury.

FILM TAIL ANCHORING CONCEPT

Early versions of AFRL blast-resistant windows (see Dover, et al. [4]) experienced "pull-out" as the glass panel marbelized and lost its ability to grip the polymer membrane (i.e., film). The pull-out produced results visually similar to the failed window in Figure 1 (although the failure mechanism in Figure 1 was different, i.e., shearing rather than pull-out). The introduction of "film tail anchoring" solved the pull-out problem with an extended edge, or "tail," on the film to provide additional gripping between the frame and panel. By using a rubber anchoring system and a film tail, the Flex window does not depend on the relatively brittle glass panels for the primary gripping force. In addition, the rubber is extended beyond the rigid frame, forming, in effect, an elastic hinge at the boundaries (earlier designs experienced a "paper cutter" effect, with broken glass causing shearing along the rigid frame edge). A schematic of the Flex window film-tail anchoring system is shown in Figure 3.

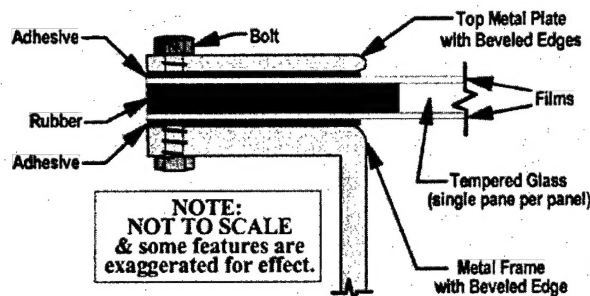


Figure 3. Flex-Retrofit Flange System

FLEX-RETROFIT FLANGE SYSTEM

The Flex-Retrofit Flange system, shown in Figure 4, is used to mount the Flex window in an existing wall. The slightly modified rigid window frame fits the existing wall with a solid flange in front and a perforated flange in back (i.e., the solid flange is bolted to the exterior of the wall, while the perforated flange is bonded to the interior of the wall using ESC). By having perforations in the flanges, there is a mechanical connection (as well as an adhesion) between the wall, the polymer, and the window flange. The combination of a solid flange in front (connected with bolts) and a perforated flange in back (connected with ESC) makes the window frame and wall act as a unit. In particular, the key result is that the window frame and wall will oscillate at the same frequency (the entire window frame can break out if they are allowed to oscillate at different frequencies).

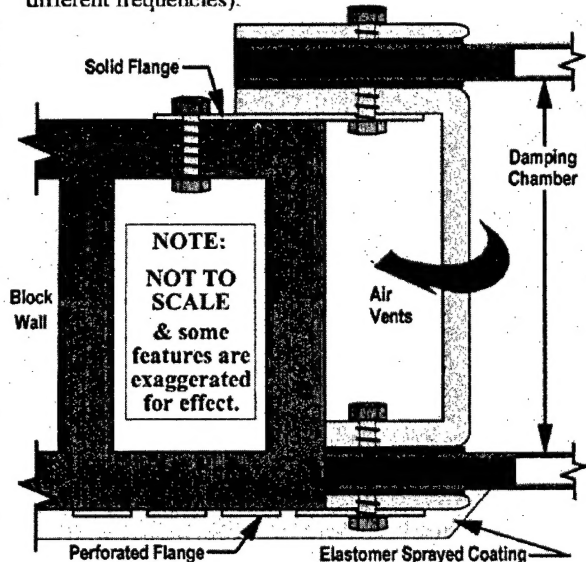


Figure 4. Flex-Retrofit Flange System

FLEX WINDOW MATERIALS

Figure 5a shows the unfinished Flex window frame, and Figure 5b shows the finished Flex window. Each Flex window has two laminated panels of glass and polymer films. While AFRL has tested a matrix of materials and

thicknesses, the general-purpose Flex window is constructed of 0.25-inch tempered glass that is bordered with butyl rubber and covered on both sides with a commercially-available safety film. The safety film is constructed of two or three layers of PETE (i.e., polyethylene terephthalate plastic), available in thicknesses of 8-mils, 14-mils, and 15-mils. The damping chamber depth was 5" (except for the wall-mounted Flex-Retrofit Flange System, which was made 7" thick to match the existing walls).

Recent testing has suggested that pre-laminated glass panes may provide additional protection when used in the Flex window, with both annealed and tempered pre-laminated glass as options. The pre-laminated panels consist of two thin glass panes, bonded to an interior polymer film during the manufacturing process. As will be shown subsequently, the marbleized shards of glass from the pre-laminated panels tend to stay attached to the inner polymer. This appears to be an advantage in the event of a "blast-after-blast"³ attack (this effect is discussed in more detail in Anderson and Dover [1]). Unfortunately, the inner film of the pre-laminated glass does not have a tail. Therefore, the pre-laminated glass is treated with safety films, with tails, to allow the tail-anchoring which creates the hinged elastic boundary condition (enabling stretching and bending at the boundary to minimize edge shear stresses).

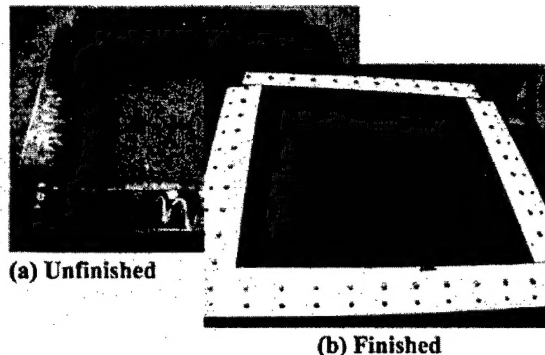


Figure 5. Basic Flex Window configuration

TESTING FLEX WINDOWS

Figure 6 shows the completed Flex window mounted in a rigid test structure (see Dover, et al. [4] for more discussion on the use, and validity, of these test devices). The rigid test structures were used in all of the tests reported herein except Target 4 (a structural retrofit). Once mounted, the windows were subjected to very high blast pressures (intended to simulate a terror bombing)

³"Blast-after-blast is a common terror technique in which a small bomb is used to draw a crowd, and a larger bomb is then used to maximize casualties.

Target No.	Shot No.	Air Gap (in.)	Panel Size (in.)			Glass Type*	Film Thick (mils)	Shock Loading Data					Interior Loading Data					
			L	W	t			(Meas.) P _{peak} (psi)	(Calc.) P _{max} (psi)	τ (ms)	I _{max} (psi-ms)	α	P _{max} (psi)	τ (ms)	t ₀ (ms)	I _{max} (psi-ms)	Z _{max}	Comments / Results
1	1	N/A	43	43	0.25	T \diamond	15	80	70	9.6	216	1.500	N/A (this was a single panel)				Failure \times	
2	1	5	43	43	0.25	T \diamond	15	98	83	9.5	237	1.764	38	8.5	21.4	98	4.130	100% Glass Retained \checkmark
3	2	5	43	43	0.25	T \diamond	15	61	58	10.5	179	1.855	26	10.3	28.2	84	3.976	100% Glass Retained
4	2	7	36	48	0.25	T \diamond	15	38	39	11.0	183	0.497	10	9.4	30.0	46	2.531	100% Glass Retained
5	3	5	43	43	0.56	PLA \dagger	15	49	50	10.6	186	1.170	19	11.1	32.7	99	2.643	100% Glass Retained
6	4	5	43	43	0.31	PLA \dagger	14	44	53	10.5	155	2.080	18	9.9	33.1	77	2.889	100% Glass Retained
7	4	5	43	43	0.25	T \diamond	15	136	144	7.2	292	2.033	63	7.8	17.1	142	4.305	Failure $\times\mathbb{X}$
8	4	5	43	43	0.25	T \diamond	8	39	40	10.4	157	0.910	22	9.0	32.7	83	2.981	Failure $\times\mathbb{X}\mathbb{X}$

* T = Tempered \times glass and film blown 25 yards down range (no damping chamber, films alone are not enough for high blast pressures)
 † PLA = Pre-Laminated Annealed \checkmark small holes in front of film, due to blast fragments (verified by high-speed videotape)
 $\mathbb{X}\mathbb{X}$ front panel sheared at boundary and blew through back panel (down range) – exceeded maximum allowable reflected pressure
 $\mathbb{X}\mathbb{X}\mathbb{X}$ both panels failed, but glass was blown up range, indicating failure during negative loading phase (i.e., during rebound)

Table 1. Summary results from Flex Window blast testing

using ANFO (i.e., Ammonium Nitrate Fuel Oil) as the “terror” explosive. The blast pressures on the windows were in excess of most civilian building codes, ranging from around 40-psi to almost 140-psi.⁴ Pressure gauges were mounted on the rigid test structures at three key locations: (1) the front face, to measure the normal reflected pressure wave; (2) inside the damping chamber, to measure the pressure build-up between panels; and (3) on the back face, to measure the “wrap-around” pressure⁵. Attempts to use strain gages to obtain supplementary data have had only moderate success, but the use of high-speed photography and videography has been a key component in assessing the Flex window’s performance.

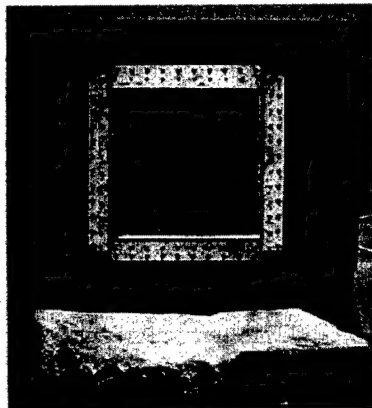


Figure 6. Flex Window in rigid test structure

TEST RESULTS

Table 1 summarizes recent testing on the Flex

⁴The typical commercially-available “blast-proof” window is rated for blast pressures less than 10-psi.

⁵The peak “wrap-around” pressure measured has typically been less than 10-psi, even for the higher peak reflected pressures.

window. The table assigns an identifying number to each target, summarizes the design / configuration for each target, summarizes the loading functions for each target (discussed at length in a subsequent section), and gives a “quick-reference” type of results summary in the “Comments / Results” column. Photographic results and more verbose descriptions are included below, summarized by “shot” (i.e., for each explosion).

SHOT 1 RESULTS

Shot 1 was a baseline test, and is shown in Figures 7 and 8, for the pre-shot and post-shot, respectively. This test was discussed previously (see Figure 1). However, the previous discussion concentrated on the shortcomings of relying on safety film (alone) for blast-protection. Having now introduced the basic concepts of the Flex window, the comparison between the two targets tested in Shot 1 becomes much more relevant. Target 2, on the right in both Figures 7 and 8, is a standard Flex window. Target 1, shown on the left in the same figures, is a standard Flex window with the back laminated panel removed. Therefore, Target 1 has the same membrane action and anchoring as a standard Flex window, but not the benefits of a damping chamber. As previously shown in Figure 1, the result is dramatic. Without a damping chamber, Target 1 becomes a projectile, despite experiencing a lower blast pressure (in fact, about 20% less measured pressure). But Target 2, the standard Flex Window, had 100% retention of glass weight (i.e., retention ratio of 100%, or RET = 1).



Figure 7. Targets 1 and 2 (pre-shot)

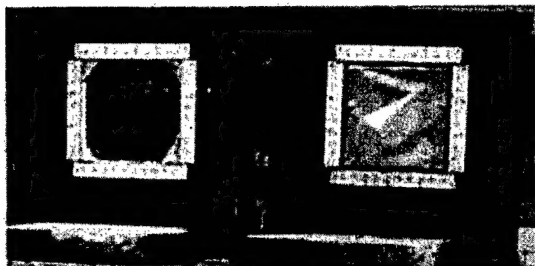
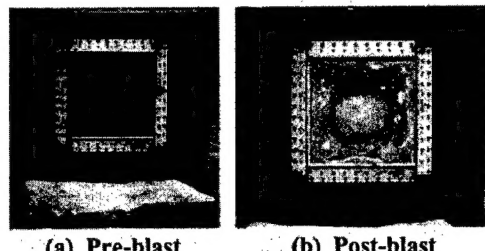


Figure 8. Targets 1 and 2 (post-shot)

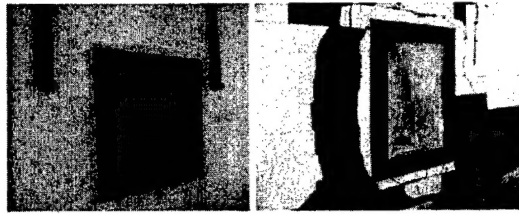
SHOT 2 RESULTS

Targets 3 and 4 were tested by Shot 2. Target 3, shown in Figure 9, was used as a control for testing of a design variation not reported herein (see Anderson and Dover [1] for discussion on the other window), so the results for that target are not particularly interesting (the previous shot had almost double the blast pressure, with 100% glass weight retained by the Flex window). On the other hand, Target 4, shown in Figure 10, presented extremely interesting results. Target 4 was a structural retrofit using the Flex-Retrofit Flange System for attachment to the existing wall (previously shown in Figure 4). More specifically, the flange system helps make the window system an integral component of the existing wall. The test for the Flex-Retrofit Flange system was intentionally severe, utilizing an existing CMU wall (concrete masonry units, or CMU, are more commonly known as "concrete blocks"). The CMU have very little tensile strength, and there is minimal reinforcement in the CMU wall system. The Flex-Retrofit Flange method is designed to be installed concurrently with an interior wall retrofit using ESC to add interior wall blast protection. The geometry of the Flex Window is adapted slightly to allow the retrofit. The front metal plate (solid flange) is bolted to the front of the wall, as well as to the rigid window frame. The back metal plate (perforated flange) is bolted to the rigid window frame, and then attached to the back of the CMU wall by ESC during the interior wall blast protection retrofit. This attachment makes the window frame and wall, as much as possible, move simultaneously (as previously discussed). Figure 10 shows the pre-blast and post-blast condition wall and the Flex-Retrofit Flange System. As expected, the window retained all of its pre-blast weight, and both panels stayed anchored to the frames. The instrumentation and videotape records show a high degree of inward deformation in the supporting structure (the CMU wall would almost certainly have fallen without the retrofit application of ESC inside the structure), yet the window was relatively unharmed. In addition, there was no apparent shearing of the exterior film, despite severe damage on the exterior surface of the CMU wall. Figure 10 is a classic example of "a picture is worth a thousand words" – the Flex window changes the structure's weakest point into its strongest.



(a) Pre-blast (b) Post-blast

Figure 9. Target 3 blast test results

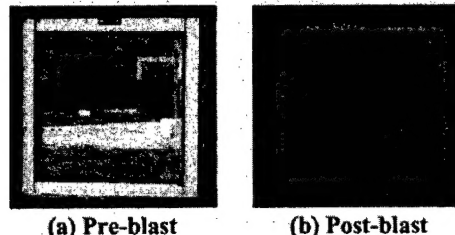


(a) Pre-blast (b) Post-blast

Figure 10. Target 4 blast test results

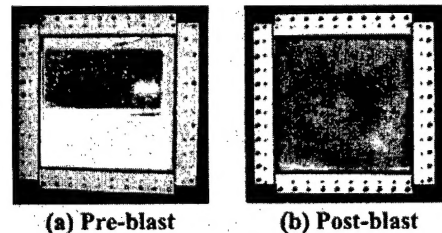
SHOT 3 AND SHOT 4 (Target 6) RESULTS

Pre-laminated glass (previously discussed) was tested in Shot 3. A thinner version of the same glass was used in Shot 4 (i.e., for Target 6), so those results are discussed in this section for the sake of clarity. Target 5, shown in Figure 11, uses pre-laminated annealed glass with two panes, each at 0.25-inch, bonded to a 0.0625-inch sheet of polyvinyl butyl (i.e., total thickness of 0.5625"). Target 6, shown in Figure 12, was also pre-laminated annealed glass, but each annealed pane was 0.125-inch thick (so that the total thickness of the pre-laminated panel was 0.3125-inch). Both Target 5 and Target 6 had 100% retention of glass weight (i.e., RET=1), and a high degree of post-blast adhesion of the marbleized shards to the inner polymer layer.



(a) Pre-blast (b) Post-blast

Figure 11. Target 5 blast test results



(a) Pre-blast (b) Post-blast

Figure 12. Target 6 blast test results

SHOT 4 (Targets 7 and 8) RESULTS

Shot 4 was an effort to test the upper limits of the Flex windows. (As previously discussed, pre-laminated panels with one-half the previous glass weight were tested in Target 6.) Target 7, shown in Figure 13, was a standard Flex window. However, to test the limits of the window, Target 7 was placed much nearer in proximity to the blast than on previous tests. For the first time the Flex window failed (but at an astonishingly high blast pressure of 137-psi). Interestingly, under this extraordinary loading, the front panel "blew out" (i.e., total shear failure near the edges), and the front panel became a projectile. The rear panel remained attached to the frame (i.e., the film anchoring worked for both panels), but was torn open by the front panel flying through it. Target 8, shown in Figure 14, attempted to substitute a thinner safety film. The standard Flex window films of 15-mil thickness were replaced with 8-mil films. Even at the lower blast pressure, the window failed. But, unlike Target 7, which "blew out" under the extreme loading, Target 8 failed on the negative phase of the blast. That is, the "blow out" was to the front of the target. This indicates that, at least after the inner glass marbelized, the already stressed 8-mil film could not resist the "pull" of the negative phase, and tore along the centerline (as clearly seen in Figure 14). In one sense, the experiment was positive, since the projection of glass shards was outward, not inward. But, the overall conclusion was that 8-mil film is not strong enough – particularly when the same basic design, but with 15-mil films, previously handled 2½ times the blast pressure on Target 8 with no loss of glass weight.

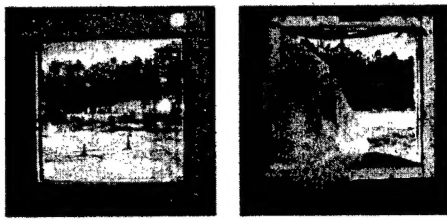


Figure 13. Target 7 blast test results

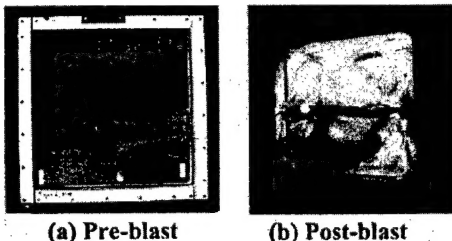


Figure 14. Target 8 blast test results

LOADING FUNCTIONS

While experimental validation via blast testing provides qualitative proof of the extraordinary abilities of

the Flex windows, modeling is needed to "fine-tune" the window's properties in a quantitative fashion. The first step in creating an accurate model of the window's behavior is to create an accurate, repeatable model of the blast loading function's positive phase. A typical exterior loading function is illustrated in Figure 15, which shows the reflected P-I Curves for Target 1 (P-I Curves are combined plots of pressure-time history and impulse-time history). A typical interior loading function is illustrated in Figure 16, which shows the internal P-I Curves for Target 6.

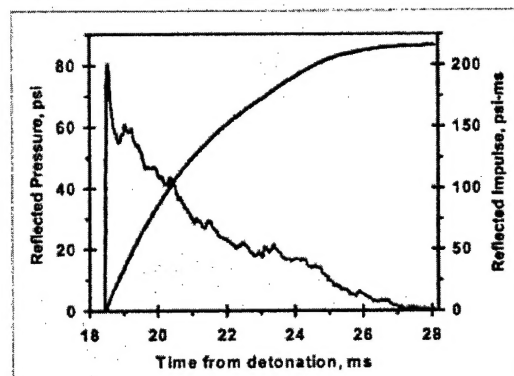


Figure 15. Typical P-I Curves, exterior loading

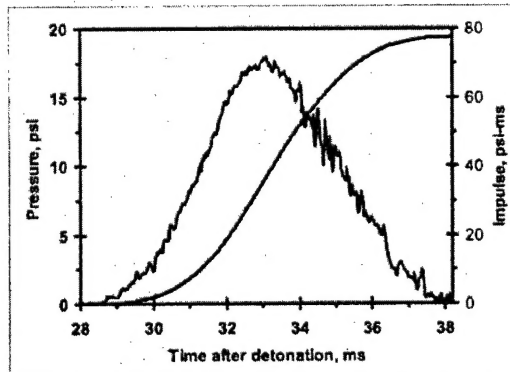


Figure 16. Typical P-I Curves, interior loading

There were several challenges in developing the best method for modeling the load functions. First, the method must provide a loading function which is relatively simple mathematically, yet repeatable physically. Second, the peak impulse of the modeled load function should match the Peak impulse of the measured load function, that is, the energy under the two pressure curves should be the same. Third, the fitted time to arrival and positive phase duration should reasonably fit the actual data (this will be even more important if future analyses consider the negative phase, as well). And, finally, the fitted curve must reasonably provide an overall good fit to the data (a constraint that is sometimes overlooked in some idealizing procedures). AFRL has developed methods of describing

the loading functions which meet all of the criteria mentioned above, although different procedures are needed for the two types of load pulses (i.e., exterior and interior), since they have different basic shapes.

MODELING THE EXTERIOR LOAD

Figure 17 explains the terms used within this section, and also illustrates the first correction step for the AFRL modeling method. The time line in Figure 17 has four key measured quantities, which are based on the raw data previously shown in Figure 15: (1) $t_{\text{detonation}}$, the time of detonation, which is the time origin for the raw data; (2) t_{arrival} , the time of first arrival of the blast wave; (3) t_{peak} , the time to the peak value of pressure; and (4) t_{final} , the time to the end of the shock wave positive phase. The pressure axis on Figure 17 has only one key measured term, P_{peak} , the highest pressure measured in the raw data.

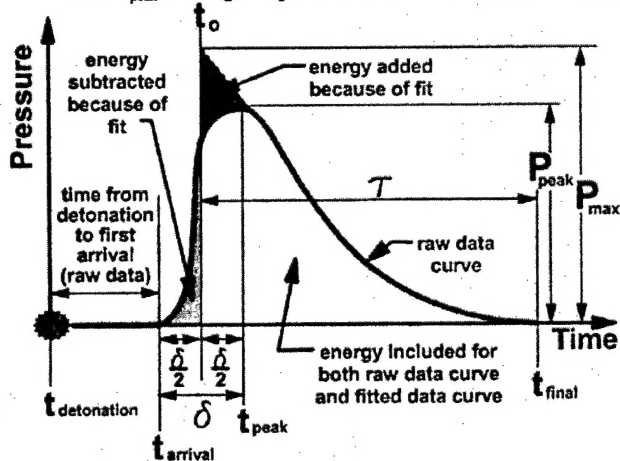


Figure 17. Graph explaining the AFRL method

The mathematical model chosen for the exterior loading function in the AFRL method is the modified Friedlander equation, expressed in Equation 1⁶, which has been shown to closely represent the shape of the exterior loading function (see, e.g., Baker [2]):

$$P(t) = P_{\text{max}} \left(1 - \frac{t}{\tau} \right) e^{-\alpha t/\tau} \quad (1)$$

where: t = time after wave arrival
 $P(t)$ = pressure at time t
 P_{max} = maximum pressure
 τ = duration of positive phase
 α = rate of decay

⁶The most rigorous form of the modified Friedlander equation also includes a term for ambient pressure, but that term is ignored herein.

Unlike Figure 15, which had the time origin at $t_{\text{detonation}}$, Equation 1 has time origin at t_o , the point where the idealized pressure is a maximum (i.e., P_{max}). Also, Equation 1 represents a "jump function" (a line of infinite slope) up to the value of P_{max} , with a subsequent reduction in pressure which depends on the rate of decay, α . This means two issues must be dealt with to produce a "good" idealized load function. First, while the theoretical equation requires an instantaneous rise to P_{max} , there is actually a finite amount of time which passes prior to registering the peak value, P_{peak} ⁷. In addition, there is a tendency for the transducer to have high-frequency "ringing" near the peak, which sometimes makes the "true" value of peak pressure (and the corresponding value, t_{peak}) difficult to determine directly. Since both of these issues tend to increase the measured time between first arrival and peak pressure, the effect of choosing the idealized time pulse origin at various locations must be considered. If t_o , the origin of the idealized load pulse, is set to the time of first arrival, t_{arrival} , then there is extra energy added to the area under the curve, which either increases the total impulse or causes a poor fit of the pressure curve down slope. Similarly, if t_o is set to t_{peak} , then energy is subtracted from the area under the curve, which either decreases the total impulse or causes a poor fit of the pressure down slope. The best model, as shown in Figure 17, would exactly balance the energy added and the energy subtracted – but such a correction would necessarily require some degree of subjectivity. The AFRL method does not exactly match these areas until later, opting instead for simplicity and objectivity in this step. Stated mathematically, the AFRL time origin correction is as follows:

$$\delta = t_{\text{peak}} - t_{\text{arrival}} \quad (2)$$

$$t_o = t_{\text{arrival}} + \frac{\delta}{2} = t_{\text{peak}} - \frac{\delta}{2} \quad (3)$$

Or, in the terms used in Figure 17, t_o is taken to be the average of t_{arrival} and t_{peak} . The calculated value of t_o then becomes the origin of the idealized time line, and the pulse duration, τ , is given by:

$$\tau = t_{\text{final}} - t_o \quad (4)$$

The second step in the AFRL modeling method is choosing the idealized value of peak pressure, P_{max} . The AFRL method uses a finding by Ethridge [5] that the initial down slope of the pressure curve tends to be very

⁷The measured time to peak has dropped dramatically with the utilization of digital pressure transducers (as compared to analog transducers), but is still typically about 20 to 30 microseconds.

linear on a semi-log plot (despite high-frequency "ringing" or other scatter in the data). The AFRL method finds P_{\max} by the following procedure: (1) the raw data (as in Figure 15) is corrected to the idealized time line by subtracting the value of t_0 , (i.e., t_0 becomes the idealized origin); (2) the linear portion⁸ of the decay curve (i.e., using only the raw data for $t \geq t_{\text{peak}}$) is fit by least-squares regression; and (3) the value of P_{\max} is the antilogarithm of the extrapolation, to the time origin, of the least-squares fit line. Figure 18 shows the application of this procedure to the data of Figure 15.

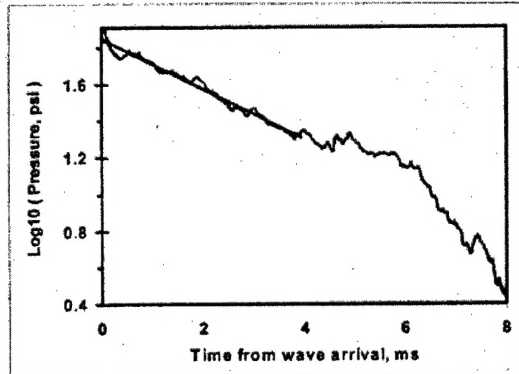


Figure 18. Correction of P_{\max}

After the first two steps, all of the terms needed for the idealized model have been obtained except for the rate of decay, α . To determine the rate of decay, the following procedure is used: (1) determine the peak impulse, I_{\max} , by numerical integration of the raw data pressure curve; (2) for simplicity, round off the values of τ , P_{\max} , and I_{\max} to the precision shown in Table 1; (3) using the theoretical expression for I_{\max} (given in Equation 5), iterate to find the value of α which matches the theoretical value of I_{\max} to the measured value of I_{\max} . The resulting fit for the data of Figure 15 is shown in Figure 19 (of course, the idealized time origin had to be shifted by t_0 to display the theoretical curve on top of the raw data). The exterior loading functions for all the tests discussed herein were determined by the AFRL method, and summarized in Table 1⁹.

$$I_{\max} = \frac{P_{\max} \tau}{\alpha} \left[1 + \left(\frac{e^{-\alpha} - 1}{\alpha} \right) \right] \quad (5)$$

⁸This step injects the only subjectivity in the AFRL method, i.e., the choice of extent of downslope that is in the "linear" range. Even so, the value of P_{\max} is not very sensitive to the range chosen, so long as the choice is "reasonable."

⁹I.e., using the Table 1 values of τ , P_{\max} , and α in the modified Friedlander equation (Equation 1) produces the idealized exterior load pulses for these tests.

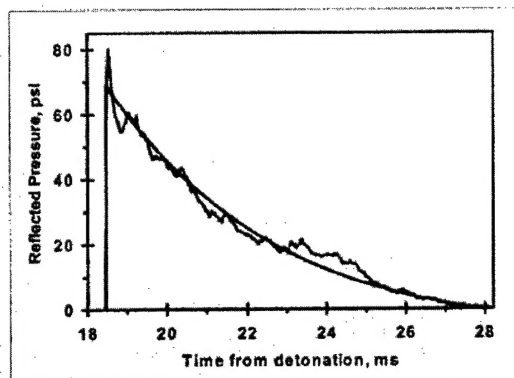


Figure 19. Idealized exterior load, AFRL method

MODELING THE INTERIOR LOAD

The AFRL method for describing the interior load function (see Figure 16) uses the assumption that the loading rate of increase is approximately equal to the rate of decay. While the symmetry is not perfect (rate of decay tends to be slightly greater than rate of increase), simplicity was the deciding factor in using this assumption in the AFRL method. In addition, the AFRL method uses the following simplifying assumptions (using terminology as in Figure 17): (1) the idealized time line has the origin at the measured peak pressure value, i.e., $t_0 = t_{\text{peak}}$; (2) the measured peak pressure is equal to the idealized peak pressure, i.e., $P_{\max} = P_{\text{peak}}$; and (3) the pulse duration is the difference in the time of arrival and the time of the end of the positive phase, i.e., $\tau = t_{\text{final}} - t_{\text{arrival}}$. Using these assumptions, the interior load pulse can be modeled with reasonable accuracy with a scaled version of the standard normal curve, expressed in general form by Equation 6 (see, e.g., Triola [7]).

$$\phi = (2\pi)^{-1/2} e^{-z^2/2} \quad (6)$$

Using the terminology of Figure 17, the idealized model equation for the interior loading function is:

$$P(t) = P_{\text{peak}} e^{-\frac{1}{2} \left[\frac{(t - t_{\text{peak}})(Z_{\max})}{(t_{\text{peak}} - t_{\text{arrival}})} \right]^2} \quad (7)$$

In terms of the values listed in Table 1, the idealized model equation for the interior loading function is:

$$P(t) = P_{\max} e^{-\frac{1}{2} \left[\frac{(t - t_0)(Z_{\max})}{\tau} \right]^2} \quad (8)$$

The key difference between the standard equation (Equation 6) and the scaled equation (Equation 7 or Equation 8) is the replacement of the standard normal

coefficient, Z , with a function of time which includes a scaling factor, Z_{\max} .¹⁰

The AFRL method for determining the idealized interior loading function is as follows: (1) find t_0 , τ , and P_{\max} as described above; (2) find the peak impulse, I_{\max} , by numerical integration of the measured interior loading function; (3) for simplicity, round the values of t_0 , τ , and P_{\max} , and I_{\max} to the precision shown in Table 1; and (4) choose a value of Z_{\max} such that the peak impulse calculated by the integration¹¹ of Equation 7 is equal to the measured peak impulse. The resulting fit for the data of Figure 16 is shown in Figure 20 (as before, the origin had to be shifted by t_0 to display the theoretical curve on top of the raw data). The interior loading functions for all the tests discussed herein were determined by the AFRL method, and summarized in Table 1.¹²

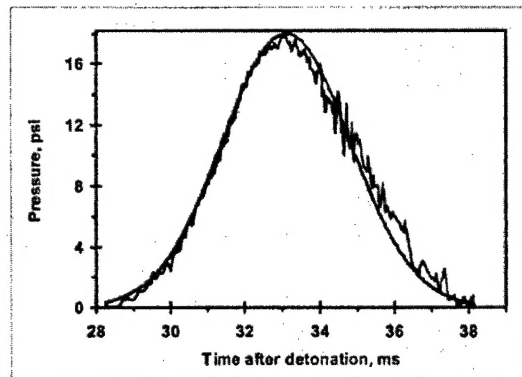


Figure 20. Idealized interior load, AFRL method

WINDOW RESPONSE MODES

To properly model the response of the Flex window, some hypothesis as to the response mode shape is needed. While AFRL has not yet quantified this behavior, there are several conclusions which can be made subjectively, based on purely observational data. Chief among these

¹⁰Mathematically, Z_{\max} refers to the point at which the values of the scaled curve (i.e., the "tails") can be considered negligible. Physically, Z_{\max} is a constant which controls the concavity of both sides of the fitted curve, i.e., Z_{\max} is related to both the rate of increase (prior to P_{\max}) and the rate of decay (after P_{\max}).

¹¹The ideal peak impulse must be calculated with a finite integration from $-\tau/2$ to $+\tau/2$ (i.e., the "tails" of the ideal function are "chopped off").

¹²I.e., using the Table 1 values of t_0 , τ , P_{\max} , and Z_{\max} in the scaled normal curve (Equation 8) produces the idealized interior load pulses for these tests.

observations is that the mode shape of the deflected window seems similar to the classic "plastic hinge" which is observed when a ductile, homogeneous, thin plate is loaded dynamically by high-speed planar waves, i.e., shock-loading. Figure 21 illustrates classic response modes for such a plate (Ross and Strickland [6]).

Despite visual observations, it is clear that the Flex window panels are neither purely ductile, nor purely homogeneous. The glass contributes a brittle component to window response, along with the elastic-plastic response of the films – and the films contribute both non-homogeneity and anisotropy. And the uncertainty is even more pronounced for tempered glass, which has high internal stresses in its unloaded state (for rapid marbleization of the glass when loaded). Without a more rigorous analysis, it would be premature to assume that the elastic-plastic-brittle behavior experienced by the Flex window can be modeled by classic elastic-plastic stress-strain equations for the plastic hinge effect. In spite of the uncertainty, however, the visual data is persuasive, particularly when observing the videotape records. Unfortunately, videotape does not lend itself to manuscript form. So, in lieu of videotape, two video frames of Target 1 are shown in Figures 22 and 23, that in combination with Figures 1 and 8, give the reader an impression of the Flex window response (also, see Figure 9b for Target 3). These figures compare favorably with Figure 24, which shows a ductile aluminum plate that was subjected to blast loading, and that was experimentally shown to fit the classic "plastic hinge" stress-strain behavior of Figure 21b (Ross and Strickland [6]).

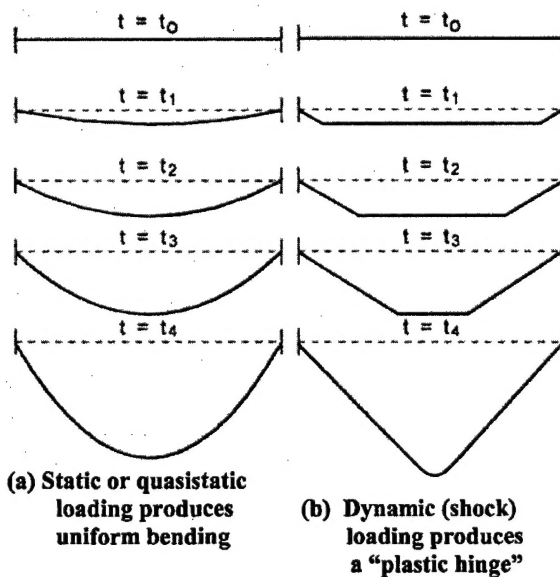


Figure 21. Classic response modes for a ductile, homogeneous, thin, square plate [6]

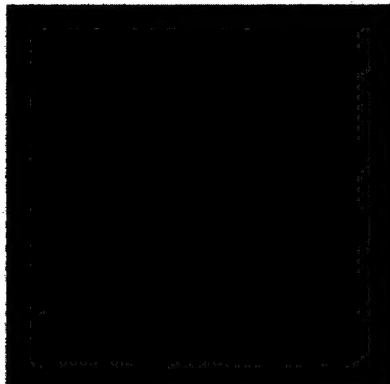


Figure 22. Target 1 response, just after loading

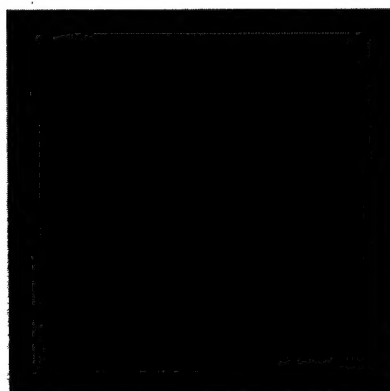


Figure 23. Target 1 response, just after failure



Figure 24. Aluminum plate after “plastic hinge” [6]

CONCLUSIONS

1. The use of protective films, alone, is not adequate protection against severe blast loading (nor are thin (i.e., 8-mil) films in any configuration).
2. The patent-pending “Blast Proof Window Systems with Damping Chamber,” better known as the AFRL Flex window, provides outstanding protection against blast loading, and is suitable for either new or retrofit construction.

3. The AFRL method provides simple mathematical equations which reasonably represent both the exterior and interior loading functions.

4. Based on visual observations, the window response mode of the Flex window appears to be the “plastic hinge” – but analytic validation is needed.

FUTURE RESEARCH

1. More research is needed on Flex windows utilizing pre-laminated panels.

2. More research is needed on the response modes of the Flex window.

3. An analytical algorithm which accurately models the response of the Flex window is needed to allow optimization of design features, such as: film thickness, size and location of vent holes, thickness of the damping chamber, and thickness of glass panes.

4. More research is needed on large-size, “store front” Flex windows (i.e., 100 ft², or greater).

5. More research is needed to characterize the PETE safety films under various loading rates and temperature regimes.

REFERENCES

- [1] Anderson, M. and Dover, D., *Sealed, Blast-resistant Windows For Retrofit Protection Against the Terrorist Threat*, Proceedings, 2nd International Conference on Innovation in Architecture, Engineering and Construction (AEC), Loughborough University, UK, June 2003.
- [2] Baker, W.E., *Explosions in Air*, University of Texas Press, Austin, Texas, 1973.
- [3] Dover, D., Anderson, M., and Brown, R.W., *Recent Advances in Matting Technology for Military Runways*, Proceedings, 27th Annual International Air Transport Conference, American Society of Civil Engineers, Orlando, Florida, July 2002.
- [4] Dover, D., Anderson, M., and Vickers, R.N., *Sealed Window Glazing System For Chemical Biological Protected Space Applications*, Proceedings, NBC Defense Collective Protection Conference (COLPRO 02), Orlando, Florida, October 2002.
- [5] Ethridge, N.H., *A Procedure for Reading and Smoothing Pressure-Time Data from H.E. and Nuclear Explosions*, BRL Memo Report No. 1691, Aberdeen Proving Ground, Maryland, 1965.
- [6] Ross, C.A. and Strickland, W.S., *Response of Flat Plates Subjected To Mild Impulsive Loadings*, The Shock And Vibration Bulletin, June 1975.
- [7] Triola, M.F., *Elementary Statistics, Eighth Edition*, Addison Wesley Longman Publishing Co., Inc., 2001.